

Stability of an Oscillon in the $SU(2)$ Gauged Higgs Model

by

Ruza Markov

Submitted to the Department of Physics
in partial fulfillment of the requirements for the degree of

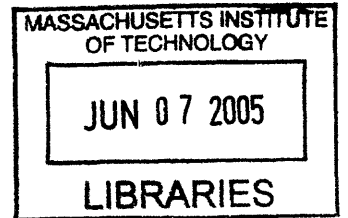
BACHELOR OF SCIENCE

at the

MASSACHUSETTS INSTITUTE OF TECHNOLOGY

Jun, 2005 [June 2005]

©2005 Ruza Markov. All Rights Reserved.



The author hereby grants to MIT permission to reproduce and to distribute publicly paper and electronic copies of this thesis document in whole or in part.

Author
Department of Physics
May 6, 2005

Certified by
Edward H. Farhi
Professor, Department of Physics
Thesis Supervisor

Accepted by
David E. Pritchard
Professor, Department of Physics
Senior Thesis Coordinator

ARCHIVES

Stability of an Oscillon in the $SU(2)$ Gauged Higgs Model

by

Ruza Markov

Submitted to the Department of Physics
on May 6, 2005, in partial fulfillment of the
requirements for the degree of
BACHELOR OF SCIENCE

Abstract

Oscillons are localized solutions of nonlinear field theories that oscillate without dissipation. We have numerically found a family of very long-lived oscillons in the spherical ansatz of the $SU(2)$ gauged Higgs model — the standard model of the weak interactions without electromagnetism and fermions. In this thesis, we study the stability of these objects. We do this by adding a massless mode to the model and coupling it to the oscillating fields contained in the Higgs doublet. Such a mode is expected to provide a decaying mechanism for the oscillons. However, numerical investigation shows that our oscillons do not decay if the massless mode is sufficiently weakly coupled and suggests that our oscillons are stable long-lived solutions that could substantially influence the dynamics of this theory.

Thesis Supervisor: Edward H. Farhi
Title: Professor, Department of Physics

Acknowledgments

I would like to thank the other Oscillators for their devoted work on this project. They are: Eddie Farhi, Noah Graham, Vishesh Khemani and Ruben Rosales. The first three chapters of this Thesis follow closely the work we published under the title *An Oscillon in the $SU(2)$ Gauged Higgs Model*.

Contents

1	Introduction	11
2	$SU(2)$ Gauged Higgs Model	13
3	Numerical Setup and Results	17
4	Stability	25
5	Conclusions	33

List of Figures

3-1	Energy density as a function of position and time (left). Total energy and energy in the box of size 80 (right).	19
3-2	Evolution of gauge invariant variables $ \phi(r=0,t) $, and $f_{01}(r=10,t)$ obtained with parameters $d_1 = -0.1$ and $d_2 = -3.2$	20
3-3	$ \phi(r,t) $ (top left), $ \chi(r,t) $ (top right), $f_{01}(r,t)$ (bottom left), and $\xi(r,t)$ (bottom right) as functions of time at different radii, for $d_1 = -0.1$ and $d_2 = -3.2$	21
3-4	The dependence of the evolution on the initial configuration. We show energy density as a function of position and time obtained with $d_1 = -0.1$ and six different values of the initial parameter d_2	22
3-5	The decay of the envelope of $ \phi $ at the origin as a function of time. The field is displayed in cyan. The maximal points of the beats (blue) are fitted with an exponential. The best fit, with $\chi^2 = 9.4$, is shown in red.	23
4-1	Time evolution of the new field, ϑ , for $c_1 = 0.06$ and $c_2 = 0.1$. ϑ as a function of r and t (left) and ϑ as a function of t for different radii (right). The field is oscillating with the beat frequency and the amplitude of these oscillations is not increasing.	27
4-2	The change of gauge invariant fields from the values they had before the new field was introduced for $c_1 = 0.06$ with $c_2 = 0.1$ (left) and $c_2 = 0.2$ (right). We show, from the top down, $ \phi(r,t) $, $ \chi(r,t) $, $f_{01}(r,t)$ and $\xi(r,t)$ as a function of time for different radii.	29

4-3	Influence of a change in coupling constant c_1 . The difference of each of the gauge invariant fields obtained with $c_1 = 0.06$ and $c_2 = -0.2$ and those obtained with $c_1 = 0.08$ and $c_2 = -0.2$, showing $ \phi(r, t) $ top left, $ \chi(r, t) $ top right, $f_{01}(r, t)$ bottom left and $\xi(r, t)$ bottom right as functions of time at different radii.	30
4-4	Influence of a change in coupling constant c_2 . The difference of each of the gauge invariant fields obtained with $c_1 = 0.06$ and $c_2 = 0.1$ and those obtained with $c_1 = 0.06$ and $c_2 = -0.2$, showing $ \phi(r, t) $ top left, $ \chi(r, t) $ top right, $f_{01}(r, t)$ bottom left and $\xi(r, t)$ bottom right as functions of time at different radii.	31

Chapter 1

Introduction

In nonlinear classical field theories, one can set up a local disturbance that would, generally, disperse away. But, sometimes, the disturbance can result in a localized solution that oscillates without dissipation. Such solutions are called *oscillons* or *breathers*.

Often, oscillons are not infinitely long-lived and only live for extremely long times. But, for physics applications, the distinction between an infinite and a very long lifetime is irrelevant. As long as the object's lifetime is significantly larger than the natural timescales of the problem, it can have significant effects on the dynamics of the theory.

We have found an oscillon in the gauged $SU(2)$ Higgs model which is the standard model of the weak interactions without electromagnetism and fermions. We worked in the spherical ansatz and numerically evolved the classical equations of motion. Even after very long runs, exceeding times of 30,000 in natural units, we have never seen this oscillon decay.

In this thesis, we study the stability of the oscillon we found. This object owes its extremely long life to its oscillation frequency which is lower than any natural mode of the system. In order to test its stability we introduce an additional effectively massless mode that provides a possible decay mechanism. We study the effects of this massless mode on the evolution of our oscillon.

Chapter 2

$SU(2)$ Gauged Higgs Model

We consider an $SU(2)$ gauge theory coupled to a doublet Higgs in $3 + 1$ dimensions, which is equivalent to the weak interactions sector of the Standard Model ignoring fermions and electromagnetism. The Lagrangian density for this theory is

$$\mathcal{L}(\mathbf{x}, t) = \left[-\frac{1}{2} \text{Tr} F^{\mu\nu} F_{\mu\nu} + \frac{1}{2} \text{Tr} (D^\mu \Phi)^\dagger D_\mu \Phi - \frac{\lambda}{4} (\text{Tr} \Phi^\dagger \Phi - v^2)^2 \right] \quad (2.1)$$

where $F_{\mu\nu} = \partial_\mu A_\nu - \partial_\nu A_\mu - ig[A_\mu, A_\nu]$, $D_\mu \Phi = (\partial_\mu - ig A_\mu) \Phi$, $A_\mu = A_\mu^a \sigma^a / 2$ and indices run over one time and three spatial dimensions. We have defined the 2×2 matrix Φ representing the Higgs doublet φ by

$$\Phi(\mathbf{x}, t) = \begin{pmatrix} \varphi_2^* & \varphi_1 \\ -\varphi_1^* & \varphi_2 \end{pmatrix}. \quad (2.2)$$

We follow the conventions of [1], except we use the metric $ds^2 = dt^2 - d\mathbf{x}^2$.

The spherical ansatz is given by expressing the gauge field A_μ and the Higgs field Φ in terms of six real functions $a_0(r, t)$, $a_1(r, t)$, $\alpha(r, t)$, $\gamma(r, t)$, $\mu(r, t)$ and $\nu(r, t)$:

$$\begin{aligned} A_0(\mathbf{x}, t) &= \frac{1}{2g} a_0(r, t) \boldsymbol{\sigma} \cdot \hat{\mathbf{x}}, \\ A_i(\mathbf{x}, t) &= \frac{1}{2g} \left[a_1(r, t) \boldsymbol{\sigma} \cdot \hat{\mathbf{x}} \hat{x}_i + \frac{\alpha(r, t)}{r} (\sigma_i - \boldsymbol{\sigma} \cdot \hat{\mathbf{x}} \hat{x}_i) + \frac{\gamma(r, t)}{r} \epsilon_{ijk} \hat{x}_j \sigma_k \right], \\ \Phi(\mathbf{x}, t) &= \frac{1}{g} [\mu(r, t) + i\nu(r, t) \boldsymbol{\sigma} \cdot \hat{\mathbf{x}}]. \end{aligned} \quad (2.3)$$

where $\hat{\boldsymbol{x}}$ is the unit three-vector in the radial direction and $\boldsymbol{\sigma}$ are the Pauli matrices.

For the fields of the full theory to be regular at the origin, a_0 , α , $a_1 - \alpha/r$, γ/r and ν must vanish as $r \rightarrow 0$. The theory reduced to this spherical ansatz has a residual $U(1)$ gauge invariance consisting of gauge transformations of the form $\exp[i\Omega(r, t)\boldsymbol{\sigma} \cdot \hat{\boldsymbol{x}}/2]$ with $\Omega(0, t) = 0$.

In the spherical ansatz we obtain the Lagrangian density

$$\begin{aligned} \mathcal{L}(r, t) = & \frac{4\pi}{g^2} \left[-\frac{1}{4} r^2 f^{\mu\nu} f_{\mu\nu} + (D^\mu \chi)^* D_\mu \chi + r^2 (D^\mu \phi)^* D_\mu \phi - \frac{1}{2r^2} (|\chi|^2 - 1)^2 \right. \\ & \left. - \frac{1}{2} (|\chi|^2 + 1) |\phi|^2 - \text{Re}(i\chi^* \phi^2) - \frac{\lambda}{g^2} r^2 \left(|\phi|^2 - \frac{g^2 v^2}{2} \right)^2 \right] \end{aligned} \quad (2.4)$$

where the indices now run over t and r and

$$\begin{aligned} f_{\mu\nu} &= \partial_\mu a_\nu - \partial_\nu a_\mu, & \chi &= \alpha + i(\gamma - 1), & \phi &= \mu + i\nu, \\ D_\mu \chi &= (\partial_\mu - ia_\mu)\chi, & D_\mu \phi &= (\partial_\mu - \frac{i}{2} a_\mu)\phi. \end{aligned} \quad (2.5)$$

Under the reduced $U(1)$ gauge invariance, the complex scalar fields χ and ϕ have charges of 1 and 1/2 respectively. a_μ is the gauge field, $f_{\mu\nu}$ is the field strength, and D_μ is the covariant derivative. The indices are raised and lowered with the 1 + 1 dimensional metric $ds^2 = dt^2 - dr^2$.

The equations of motion for the reduced theory are

$$\begin{aligned} \partial^\mu (r^2 f_{\mu\nu}) &= i [D_\nu \chi^* \chi - \chi^* D_\nu \chi] + \frac{i}{2} r^2 [D_\nu \phi^* \phi - \phi^* D_\nu \phi], \\ i\chi\phi^* &= \left[D^\mu r^2 D_\mu + \frac{1}{2} (|\chi|^2 + 1) + \frac{2\lambda}{g^2} r^2 \left(|\phi|^2 - \frac{g^2 v^2}{2} \right) \right] \phi, \\ -\frac{i}{2} \phi^2 &= \left[D^2 + \frac{1}{r^2} (|\chi|^2 - 1) + \frac{1}{2} |\phi|^2 \right] \chi. \end{aligned} \quad (2.6)$$

These equations can be obtained either by varying the Lagrangian density (2.4) or by imposing the spherical ansatz on the equations of motion of the full theory.

Although the theory is described by six fields, a_0 , a_1 , μ , ν , α , and γ , there are only four independent degrees of freedom consisting of the three W -bosons and the massive Higgs. The remaining degrees of freedom are gauge artifacts. We may fix

the gauge by a time-dependent gauge transformation followed by a time-independent gauge transformation which removes the remaining gauge freedom. We choose to first set $a_0(r, t) = 0$ everywhere, and then apply a time-independent gauge transformation to set $a_1(r, t = 0) = 0$ initially. The choice of $a_0 = 0$ gauge makes the covariant time derivatives equal to the regular time derivatives.

As we chose $a_0 = 0$ there are only five fields that evolve in time. To obtain time evolution, for each of the four fields μ , ν , α , and γ we must specify the profile at $t = 0$ as a function of r as well as the time derivative of the profile at $t = 0$ as a function of r . The time derivative of $a_1(r, t)$ at $t = 0$ is then determined by imposing Gauss's Law which is the first equation in (2.6) with index $\nu = 0$. In this gauge, Gauss's Law is

$$\begin{aligned} \partial_r(r^2 \partial_t a_1(r, t)) &= \frac{r^2}{2i} [\phi(r, t)^* \partial_t \phi(r, t) - \partial_t \phi(r, t)^* \phi(r, t)] \\ &\quad + \frac{1}{i} [\chi(r, t)^* \partial_t \chi(r, t) - \partial_t \chi(r, t)^* \chi(r, t)]. \end{aligned} \quad (2.7)$$

We evolve these five fields according to the Equations (2.6). Configurations obeying Gauss's Law at the initial time will obey it for all times. Thus we have fully specified the initial value problem by providing initial value data for the four real degrees of freedom contained in μ , ν , α , and γ .

Chapter 3

Numerical Setup and Results

In order to accurately simulate the extremely long lifetimes of oscillons, we require highly stable numerical techniques. We discretize the system at the level of the Lagrangian in Equation (2.4). We choose a fixed spatial lattice spacing Δr , placing the scalar fields at the sites of the lattice and the gauge field a_1 on the links. Thus each of the five scalar fields $\lambda(r, t)$ is replaced by a set of functions $\lambda^{\{n\}}(t)$, defined at each lattice point. Further on, we replace a first-order lattice gauge-covariant derivative by the discrete expression

$$D_r \lambda(r, t) \longrightarrow \frac{\lambda^{\{n+1\}}(t) \exp[-iga_1^{\{n+\frac{1}{2}\}}(t)\Delta r] - \lambda^{\{n\}}(t)}{\Delta r} \quad (3.1)$$

where g is the charge of the scalar field λ and $n = r/\Delta r$ labels the lattice point corresponding to radius r .

We vary the spatially discretized Lagrangian to obtain second-order accurate lattice equations of motion. In the limit of continuum time evolution, this system has *exact* conservation of energy and exact gauge invariance. We monitor these quantities to detect numerical errors and determine whether our time steps are short enough. However, they do not tell us whether our spatial grid is fine enough, because even for a very coarse grid our system conserves energy and obeys Gauss's Law. In all our simulations, these invariants hold to an accuracy of roughly one part in 10^6 , and we see no numerical instabilities even after extremely long runs.

Since we chose to work in a $a_0(r, t) = 0$ gauge, the covariant time derivative coincides with the ordinary time derivative. Thus, the discrete second-order time derivative is given by

$$D_t^2 \lambda(r, t) \longrightarrow \frac{\lambda^{\{n\}}(t + \Delta t) - 2\lambda^{\{n\}}(t) + \lambda^{\{n\}}(t - \Delta t)}{(\Delta t)^2}. \quad (3.2)$$

Our time evolution is simply inverting this second-order differential, which appears in the equations of motion, in order to solve for $\lambda^{\{n\}}(t + \Delta t)$. Thus, we compute each new time step from the previous two. This approach is stable for $\Delta t < \Delta r$ so we choose to work with a fixed time step $\Delta t = \Delta r/2$.

In order to monitor the energy conservation and gauge invariance of the solution, it is necessary to compute first-order time derivatives. We compute the derivative at time t_0 by subtracting the result at $t_0 - \Delta t$ from the result at $t_0 + \Delta t$ and dividing by $2\Delta t$, rather than comparing adjacent time steps t_0 and $t_0 + \Delta t$. We chose this definition of the first derivative because, in the continuum limit, it is accurate to the second order in Δt unlike the one using adjacent time steps which is only accurate to the first order.

Since we are considering classical dynamics, the theory is invariant under overall rescalings of the Lagrangian density. As a result, the theory is completely specified by the choice of the ratio of the Higgs mass $m_H = v\sqrt{2\lambda}$ to the W -boson mass $m_W = gv/2$. For generic values of this ratio, we observe localized configurations that oscillate but are spreading out and decaying. However, in a particular case $m_H = 2m_W$ these oscillations exhibit no observable decay in our simulation. This is the only mass ratio at which we found stable oscillons in this theory. We chose to work with $g = \sqrt{2}$ and $\lambda = 1$ which give this mass ratio. Also, we chose to work in natural units with the vacuum expectation value of the ϕ field $v = 1$.

The localized initial configuration we start from is given by

$$\phi(r, t = 0) = \frac{gv}{\sqrt{2}} \left(1 + d_1 e^{-r^2/w^2}\right) \quad \text{and} \quad \chi(r, t = 0) = -i \left(1 + id_2 e^{-r^2/w^2}\right) \quad (3.3)$$

where d_1 , d_2 , and w parameterize the initial configuration. We set initial time deriv-

atives equal to zero everywhere. Then, we evolve this configuration according to the equations of motion and observe its evolution. To ensure that we are not seeing numerical artifacts we monitor gauge-invariant quantities. A clear choice are the energy and energy density. As described in [1], there are also four gauge-invariant field $|\phi(r,t)|$, $|\chi(r,t)|$, $f_{01}(r,t)$, and $\xi(r,t) = \arg [i\chi(r,t)(\phi(r,t))^*]$, that completely determine the state of the system.

We display results for $d_1 = -0.1$, $d_2 = -3.2$, and $w = 12$ although small changes in these parameters give similar results. In the left panel of Figure 3-1 we show the energy density as a function of t and r . A localized time dependent object is clearly visible. The right panel shows that the initial configuration sheds about a quarter of its energy and quickly settles into the localized oscillon which does not decay visibly.

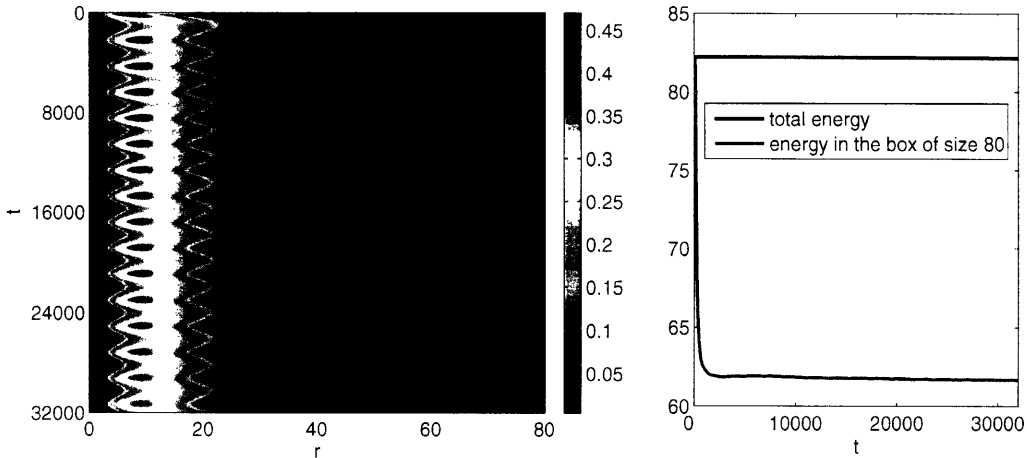


Figure 3-1: Energy density as a function of position and time (left). Total energy and energy in the box of size 80 (right).

In the upper left panel of Figure 3-2 we show the gauge invariant magnitude of ϕ at the origin, $|\phi(r=0,t)|$. The field is oscillating about the vacuum expectation value at $\phi = v = 1$. By counting the number of oscillations, the frequency of the oscillation is measured to be 0.2239. As the mass of the Higgs is $\sqrt{2}$ the lowest frequency of any propagating mode of the Higgs field is $\sqrt{2}/2\pi = 0.2251$ which is above the oscillon frequency. This is an essential property. Any oscillon owes its long life to a frequency of oscillation which is below any natural mode of the system. Such an object cannot

decay into modes which can carry energy away.

We also show that the gauge invariant quantity $f_{01}(r = 10, t)$ is oscillating with a frequency of 0.1120 --- exactly half of the frequency of oscillations of $|\phi|$ within the accuracy of the measurement. The gauge boson mass is $\sqrt{2}/2$ so the lowest frequency of these propagating modes is $\sqrt{2}/4\pi = 0.1125$ which is also above the oscillation frequency. Similar analysis holds for the other two gauge invariant fields, $|\chi(r, t)|$ and $\xi(r, t)$ where $|\chi(r, t)|$ oscillates with same frequency as $|\phi(r, t)|$ while $\xi(r, t)$ oscillates with same frequency as $f_{01}(r, t)$.

In the lower panels of Figure 3-2 we plot the two fields over a much longer time so that their oscillations are not visible. However we do see beats in these profiles. The beat frequency of both fields is about 4.8×10^{-1} .

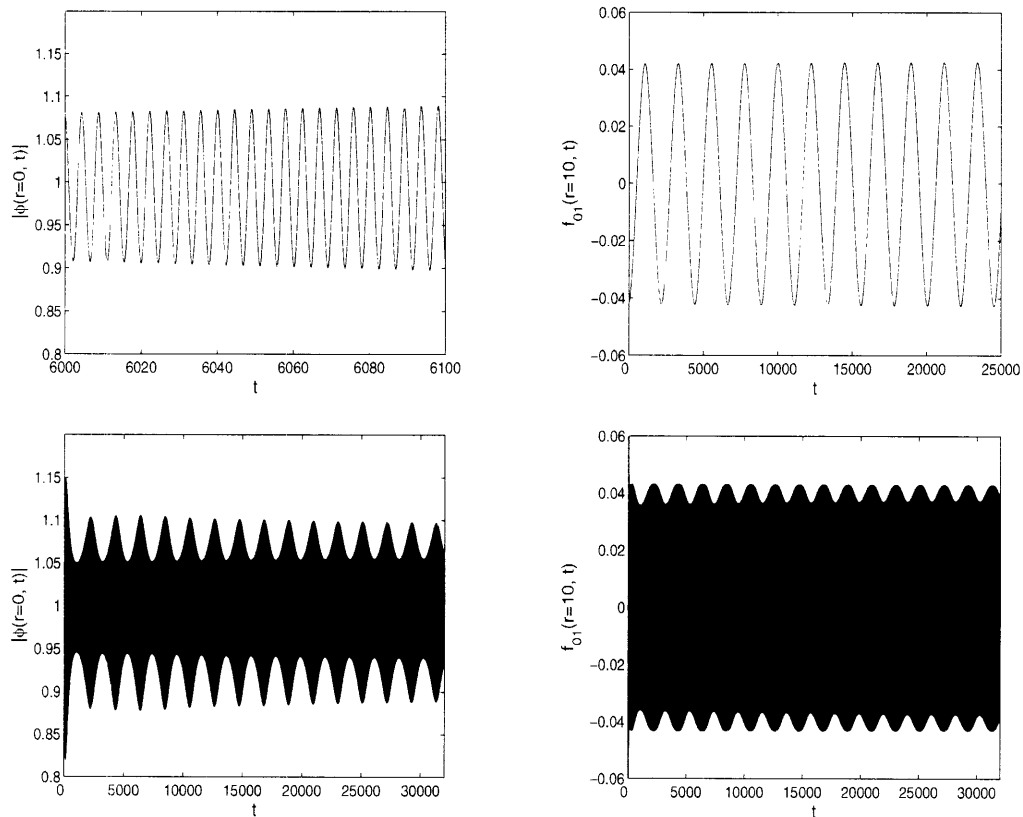


Figure 3-2: Evolution of gauge invariant variables $|\phi(r = 0, t)|$, and $f_{01}(r = 10, t)$ obtained with parameters $d_1 = -0.1$ and $d_2 = -3.2$.

In Figure 3-3 we show the profiles of four gauge invariant fields, $|\phi(r, t)|$, $|\chi(r, t)|$, $f_{01}(r, t)$, and $\xi(r, t) = \arg [i\chi(r, t)(\phi(r, t)^*)^2]$, as a function of time for four different radii.

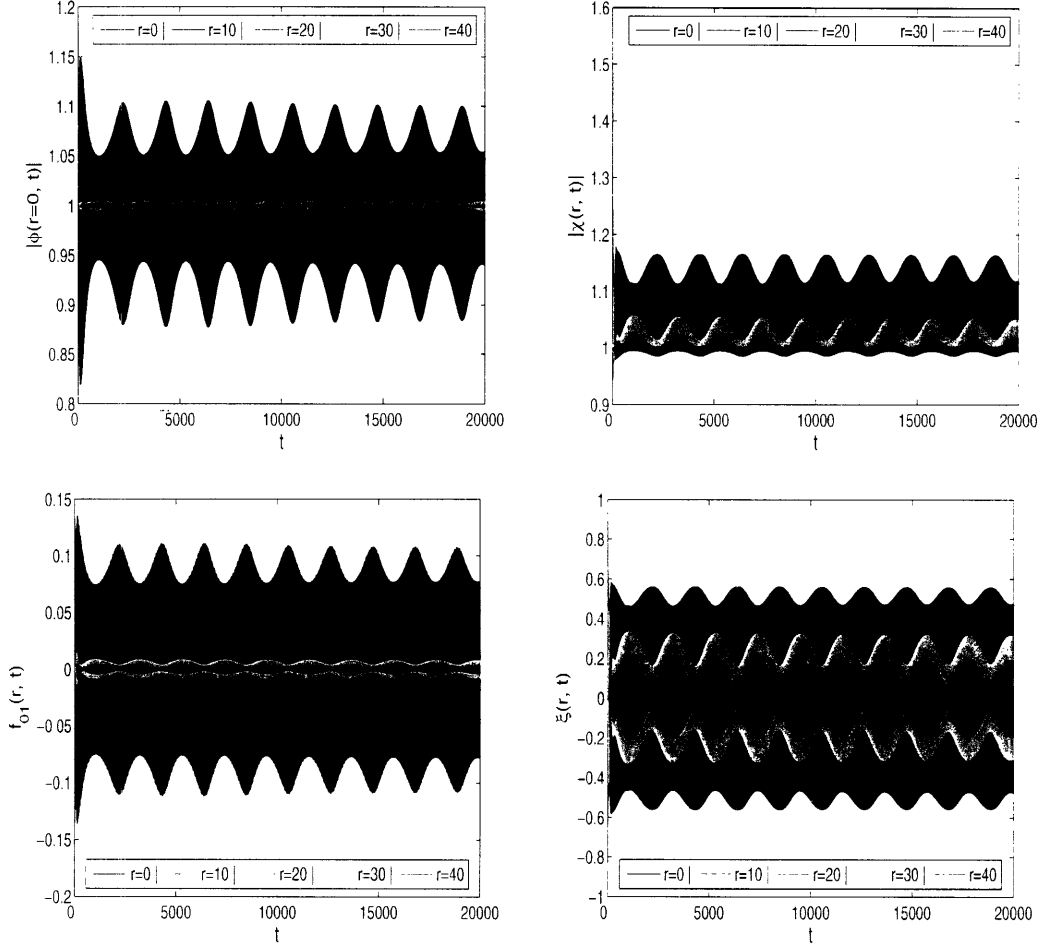


Figure 3-3: $|\phi(r, t)|$ (top left), $|\chi(r, t)|$ (top right), $f_{01}(r, t)$ (bottom left), and $\xi(r, t)$ (bottom right) as functions of time at different radii, for $d_1 = -0.1$ and $d_2 = -3.2$.

Although a particular initial configuration is displayed, the details of the starting point are not essential. In the beginning, the initial configuration varies substantially. It sheds energy and finally settles into the stable configuration. From the left panel of Figure 3-1 one can see energy leaving the small region around the origin during the shedding. The fact that our initial configuration spontaneously settles into an oscillon could mean that oscillons can form from generic initial conditions and are

not improbable solutions.

However, changing the initial conditions does affect the nature of the oscillation. In Figure 3-4 we show that the beat frequency of the oscillon depends on the initial configuration. There, parameter d_2 is varied until the oscillon becomes unstable.

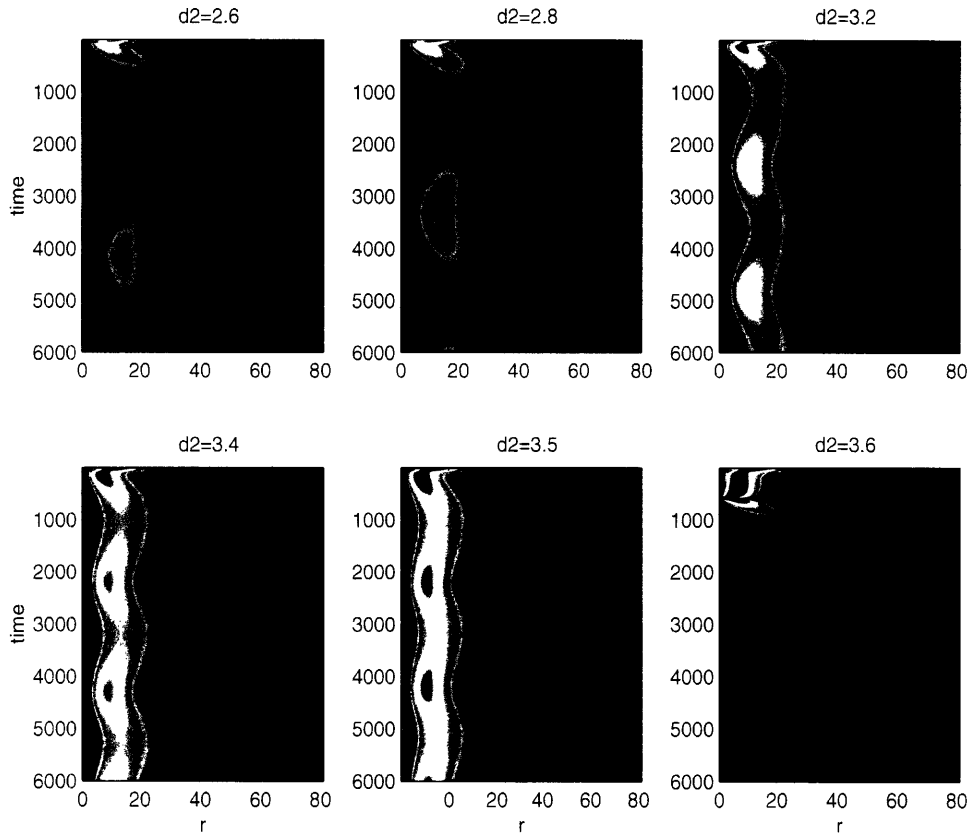


Figure 3-4: The dependence of the evolution on the initial configuration. We show energy density as a function of position and time obtained with $d_1 = -0.1$ and six different values of the initial parameter d_2 .

We never saw the death of the oscillon shown in Figures 3-1, 3-2 and 3-3. But, a careful eye can notice a slight decay in the maximal value that the beats of the fields achieve. This effect is displayed in cyan in Figure 3-5 for $|\phi|$ at the origin, where the vertical axis is stretched until this decay is clearly visible. This figure also shows that there is a beat in the beats of this field.

The maximal points of the beats of $|\phi(r, t)|$ at the origin were read off and fitted with a shifted exponential function of time, $ae^{-bt} + c$, where $c = 1$ is the vacuum

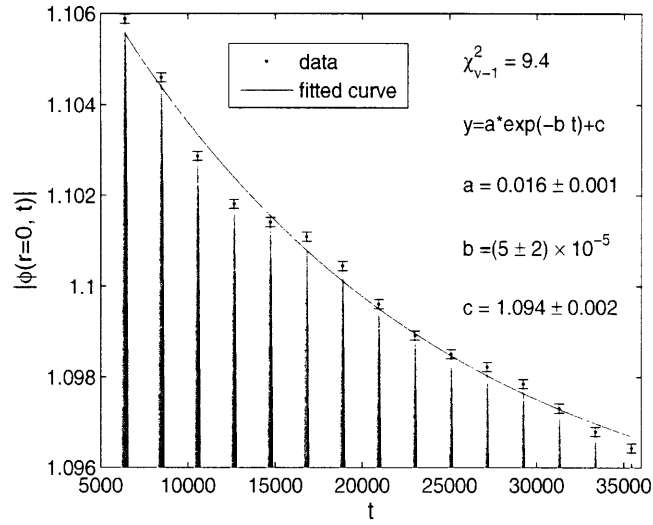


Figure 3-5: The decay of the envelope of $|\phi|$ at the origin as a function of time. The field is displayed in cyan. The maximal points of the beats (blue) are fitted with an exponential. The best fit, with $\chi^2 = 9.4$, is shown in red.

value. The fitted curve and its parameters are shown in Figure 3-5, as well. Although the decay rate, $b = (5 \pm 2) \times 10^{-5}$, could not be determined very precisely due to insufficient data, the constant offset, $c = 1.094 \pm 0.002$ is determined with relative error of less than 0.2%. The fact that this offset does not equal the vacuum expectation value $v = 1$ suggests that the oscillon is not decaying but only settling into a stable configuration.

Chapter 4

Stability

In order to study the stability of the oscillon described in Chapter 3 we introduce a massless scalar field ϑ coupled to the Higgs doublet. This is a good check of the robustness of our object as an uncoupled oscillon owes its long life to the fact that its frequency of oscillation is lower than any natural mode of the system, so there are no modes that can carry its energy away. The addition of a massless field may provide a decay mechanism for the oscillon.

The new Lagrangian we choose is

$$\begin{aligned} \mathcal{L}(\mathbf{x}, t) = & \left[-\frac{1}{2} \text{Tr} F^{\mu\nu} F_{\mu\nu} + \frac{1}{2} \partial^\mu \vartheta \partial_\mu \vartheta + \frac{1}{2} \text{Tr} (D^\mu \Phi)^\dagger D_\mu \Phi \right. \\ & \left. - \frac{1}{4} (\lambda - c_1 \vartheta - c_2 \vartheta^2) (\text{Tr} \Phi^\dagger \Phi - v^2)^2 \right] \end{aligned} \quad (4.1)$$

which reduces to the Lagrangian in equation (2.1) when $\vartheta(\mathbf{x}, t) = 0$ everywhere.

In the spherical ansatz this Lagrangian is

$$\begin{aligned} \mathcal{L}(r, t) = & \frac{4\pi}{g^2} \left[-\frac{1}{4} r^2 f^{\mu\nu} f_{\mu\nu} + (D^\mu \chi)^* D_\mu \chi + r^2 (D^\mu \phi)^* D_\mu \phi + \frac{g^2 r^2}{2} \partial^\mu \vartheta \partial_\mu \vartheta \right. \\ & - \frac{1}{2r^2} (|\chi|^2 - 1)^2 - \frac{1}{2} (|\chi|^2 + 1) |\phi|^2 - \text{Re}(i \chi^* \phi^2) \\ & \left. - \frac{r^2}{g^2} (\lambda - c_1 \vartheta - c_2 \vartheta^2) \left(|\phi|^2 - \frac{g^2 v^2}{2} \right)^2 \right] \end{aligned} \quad (4.2)$$

with the indexes running over t and r and all the fields depending only on r and t .

as defined in Chapter 2. The regularity of this theory at $r = 0$ implies that $\partial\vartheta/\partial r$, a_0 , α , $a_1 - \alpha/r$, γ/r and ν must vanish as $r \rightarrow 0$.

The equations of motion for this spherical Lagrangian are

$$\begin{aligned}
\partial^\mu(r^2 f_{\mu\nu}) &= i[D_\nu \chi^* \chi - \chi^* D_\nu \chi] + \frac{i}{2} r^2 [D_\nu \phi^* \phi - \phi^* D_\nu \phi], \\
i\chi \phi^* &= \left[D^\mu r^2 D_\mu + \frac{1}{2}(|\chi|^2 + 1) + \frac{2r^2}{g^2} (\lambda - c_1 \vartheta - c_2 \vartheta^2) \left(|\phi|^2 - \frac{g^2 \vartheta^2}{2} \right) \right] \phi, \\
-\frac{i}{2} \phi^2 &= \left[D^2 + \frac{1}{r^2} (|\chi|^2 - 1) + \frac{1}{2} |\phi|^2 \right] \chi, \\
\partial^\mu(r^2 \partial_\mu \vartheta) &= \frac{2r^2}{g^4} (c_1 + 2c_2 \vartheta) \left(|\phi|^2 - \frac{g^2 \vartheta^2}{2} \right)^2. \tag{4.3}
\end{aligned}$$

Again, we will fix the gauge by first setting $a_0(r, t) = 0$ everywhere, and then applying a time-independent gauge transformation to set $a_1(r, t = 0) = 0$ initially. To obtain time evolution, for each of the five real fields μ , ν , α , γ , and ϑ we must specify the profile at $t = 0$ as a function of r as well as the time derivative of the profile at $t = 0$ as a function of r . The time derivative of $a_1(r, t)$ at $t = 0$ is then determined by imposing Gauss's Law, the first equation in (4.3) with index $\nu = 0$, which in this gauge reads:

$$\begin{aligned}
\partial_r(r^2 \partial_t a_1(r, t)) &= \frac{r^2}{2i} [\dot{\phi}(r, t)^* \partial_t \phi(r, t) - \partial_t \phi(r, t)^* \dot{\phi}(r, t)] \\
&\quad + \frac{1}{i} [\chi(r, t)^* \partial_t \chi(r, t) - \partial_t \chi(r, t)^* \chi(r, t)]. \tag{4.4}
\end{aligned}$$

We evolve the five fields according to equations (4.3) and the configurations obeying Gauss's Law at the initial time then obey it for all times. Thus we have fully specified the initial value problem by providing initial value data for the five real degrees of freedom contained in μ , ν , α , γ , and ϑ , corresponding to the five degrees of freedom of this theory.

In order to see how the newly introduced field ϑ influences the stability of our oscillons we choose the same initial configuration for μ , ν , α , and γ as the one that gave rise to an oscillon. We arbitrarily choose the oscillon with $d_1 = -0.1$ and $d_2 = -3.2$ as the essential properties of the oscillons did not depend on the initial

configuration. Also, we choose a static initial configuration for the new field given by $\vartheta(r) = 0$. $\partial\vartheta(r)/\partial t = 0$. From the last equation in (4.3) we see that if $c_1 \neq 0$ this static zero field configuration will evolve and move away from zero.

We are interested in knowing if the new field ϑ carries energy away from the oscillon. Because the system now has a natural mode lower than the frequency of oscillation of the oscillon we think that energy will be transferring from the oscillon to the massless field. As a massless mode cannot keep the energy confined, we expect to see the energy dissipating out of the small region near the origin.

Figure 4-1 shows the evolution of ϑ for $c_1 = 0.06$ and $c_2 = 0.1$. The initial static zero field evolves and pulses with the frequency of the beats in the other fields. The amplitude and frequency of these pulses is not changing in time. This shows that although there is some energy stored in the new field, contrary to our expectations this amount is not increasing in time. The energy is not continuously transferring from the massive fields to the massless field. After the oscillon has stabilized, the energy in the box of size 80 is 61.6 in this case while it was 61.8 before ϑ was introduced.

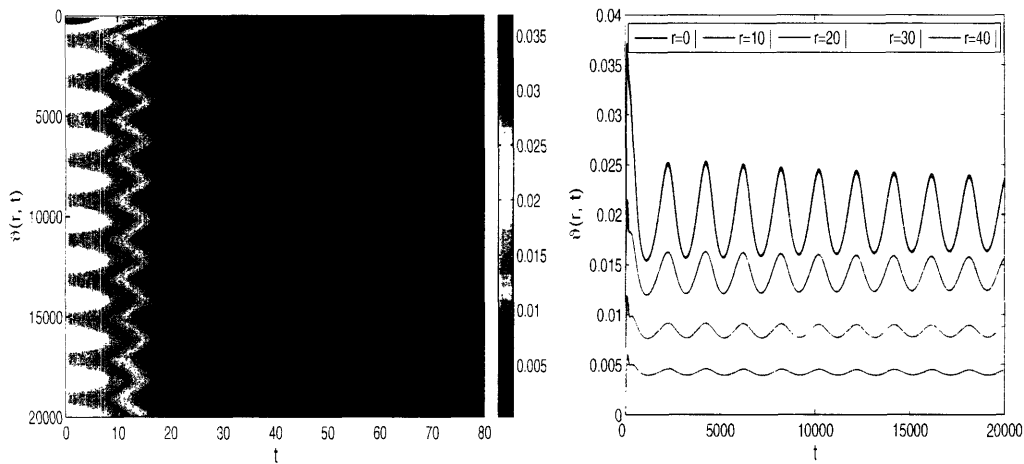


Figure 4-1: Time evolution of the new field, ϑ , for $c_1 = 0.06$ and $c_2 = 0.1$. ϑ as a function of r and t (left) and ϑ as a function of t for different radii (right). The field is oscillating with the beat frequency and the amplitude of these oscillations is not increasing.

In order to see how the new evolving massless mode effects the evolution of the other fields we compare the gauge invariant variables without the new field (or, equiv-

alently, with $c_1 = 0$ and $c_2 = 0$) and with ϑ present, as illustrated in Figure 4-2. The right column is the difference of the results obtained with $c_1 = 0.06$, $c_2 = 0.1$ and those with no ϑ while the left column compares the results obtained with $c_1 = 0.06$ and $c_2 = -0.2$ to those with no ϑ . Row by row, from top to bottom, we show the change of $|\phi(r, t)|$, $|\chi(r, t)|$, $f_{01}(r, t)$ and $\xi(r, t)$. We see that the change in the fields is quasi-periodic and does not grow in time. The 'period' of this quasi-periodic evolution of $f_{01}(r, t)$ and $\xi(r, t)$ is twice that for $|\phi(r, t)|$ and $|\chi(r, t)|$. We also see that the 'period' is longer for $c_2 = -0.2$ than $c_2 = 0.1$.

The dependence on the coupling constant c_1 is shown in Figure 4-3, where we plot the difference of each of the four gauge invariant fields obtained with different coupling constant c_1 and the same c_2 . Specifically, we used $c_2 = -0.2$ and $c_1 = 0.06$ for one run while $c_1 = 0.08$ for the other, and plotted the difference between the gauge invariant fields between these two runs. We see that the difference between the fields is, on average, not growing in time, but is periodic and oscillates around zero. The period of this oscillation for $|\phi(r, t)|$ and $|\chi(r, t)|$ is the same and very nearly equals half of that for $f_{01}(r, t)$ and $\xi(r, t)$.

Figure 4-2 shows that the changes in the fields due to introducing ϑ with the two different values of c_2 are very similar. Results obtained with $c_2 = 0.1$ and $c_2 = -0.2$ (both having $c_1 = 0.06$) are directly compared in Figure 4-4, where we plot the difference of each of the four gauge invariant fields obtained with different coupling constant c_2 . We see that the amount by which $|\phi(r, t)|$ and $|\chi(r, t)|$ differ for $c_2 = 0.1$ and $c_2 = -0.2$ is growing at first and then decreasing after a time of about 15000 suggesting that it actually oscillates with period of about 30000. On the other hand, amounts by which $f_{01}(r, t)$ and $\xi(r, t)$ differ is growing over the time of the run of 20000, but the properties noticed above suggest that they are actually quasi-periodic with period of about 60000. A longer run is necessary to further test the dependence on the coupling constant c_2 .

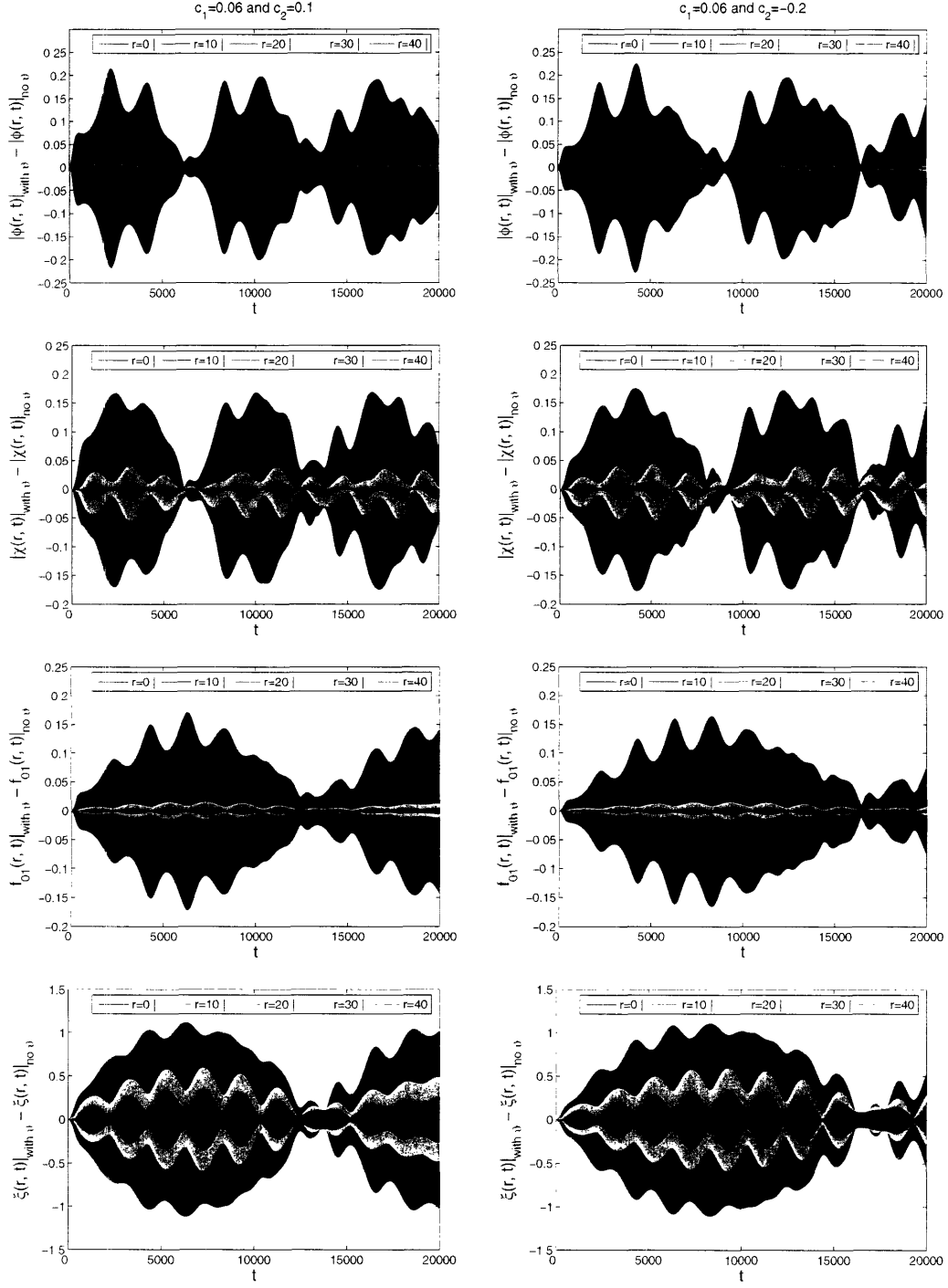


Figure 4-2: The change of gauge invariant fields from the values they had before the new field was introduced for $c_1 = 0.06$ with $c_2 = 0.1$ (left) and $c_2 = 0.2$ (right). We show, from the top down, $|\phi(r,t)|$, $|\lambda(r,t)|$, $f_{01}(r,t)$ and $\xi(r,t)$ as a function of time for different radii.

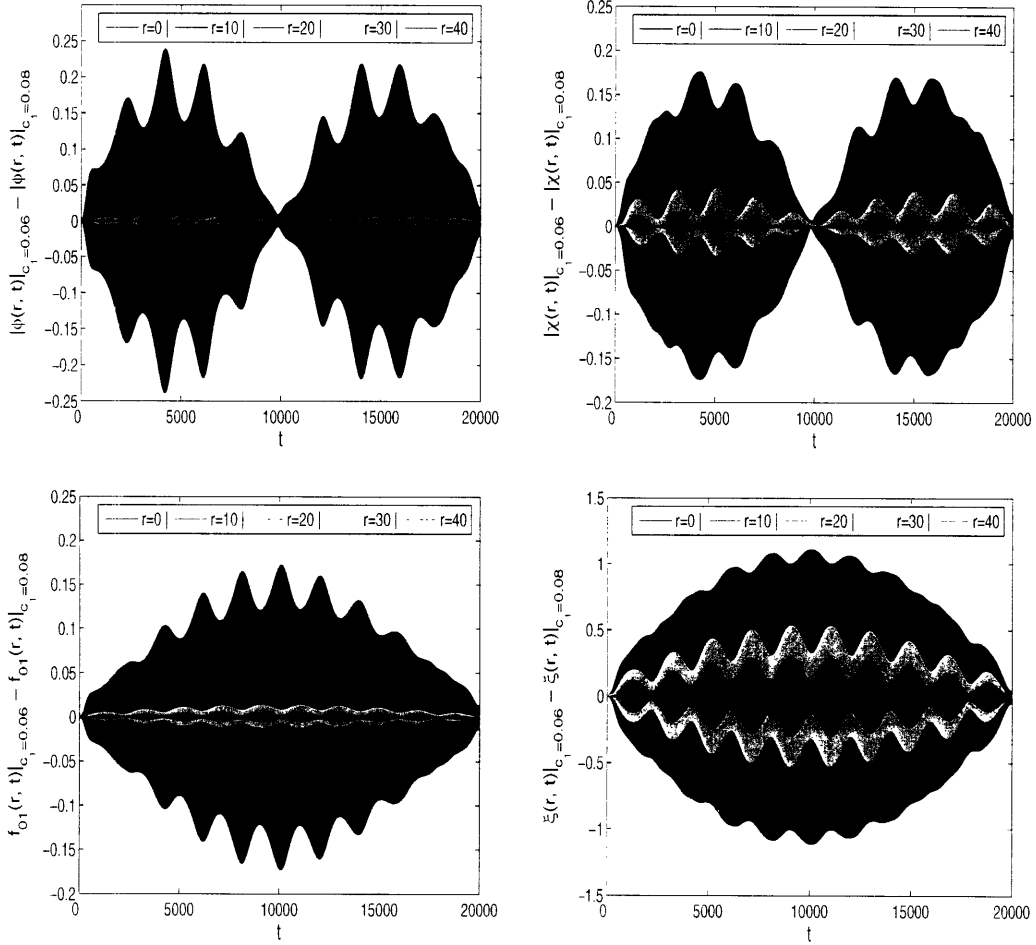


Figure 4-3: Influence of a change in coupling constant c_1 . The difference of each of the gauge invariant fields obtained with $c_1 = 0.06$ and $c_2 = -0.2$ and those obtained with $c_1 = 0.08$ and $c_2 = -0.2$, showing $|\phi(r, t)|$ top left, $|\chi(r, t)|$ top right, $f_{01}(r, t)$ bottom left and $\xi(r, t)$ bottom right as functions of time at different radii.

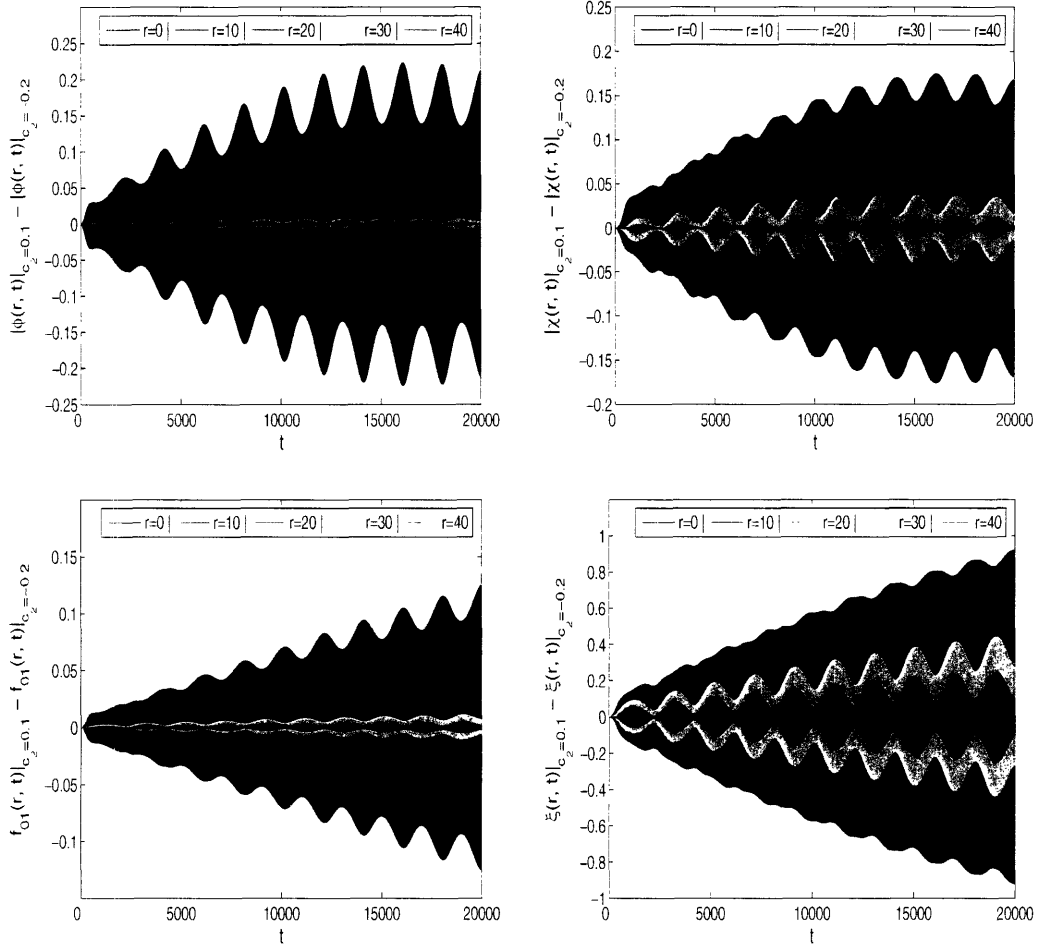


Figure 4-4: Influence of a change in coupling constant c_2 . The difference of each of the gauge invariant fields obtained with $c_1 = 0.06$ and $c_2 = 0.1$ and those obtained with $c_1 = 0.06$ and $c_2 = -0.2$, showing $|\phi(r, t)|$ top left, $|\chi(r, t)|$ top right, $f_{01}(r, t)$ bottom left and $\xi(r, t)$ bottom right as functions of time at different radii.

Chapter 5

Conclusions

In this Thesis we studied the stability of an oscillon in the $SU(2)$ gauged Higgs model by introducing a massless field coupled to the oscillating Higgs doublet. Contrary to our expectations we found that a sufficiently weakly coupled massless field does not destabilize the oscillon. We saw that only a small amount of energy is transferred to the new field and that this amount does not grow in time. We also saw that the new field does not introduce an increasing change in the gauge invariant fields describing the state of the system. This suggests that our oscillon is a stable long-lived solution which can substantially influence the dynamics of this theory.

The next natural question is: how does this finding depend on the strength of the coupling? How strong must the coupling be for the oscillon to become unstable? We did not pursue this issue as our numerical simulation becomes unstable for larger couplings -- the results stop obeying Gauss's Law and conserving energy. Further investigation is needed to find the source of this numerical instability. Then, the robustness of the oscillon could be tested for a strongly coupled massless field.

Bibliography

- [1] E. Farhi, K. Rajagopal, and R. Singleton, hep-ph/9503268. Phys. Rev. **D52** (1995) 2394.
- [2] R. Rajaraman. *Solitons and Instantons* (North-Holland, Amsterdam, 1982).
- [3] C. Nash and S. Sen. *Topology and Geometry for Physicists*. (Academic Press, London, 1983).